

# The Influence of Heat Treatment on the Phase Structure of the Nanocrystalline $(\text{Nd}_{10}\text{Fe}_{67}\text{B}_{23})_{95}\text{Nb}_5$ Alloy Ribbons

IZABELA WNUK\*, MALGORZATA SZWAJA

Department of Physics, Czestochowa University of Technology, Armii Krajowej 19, 42-200 Czestochowa, Poland

*The main goal of present paper was to study of phase composition of nanocrystalline  $(\text{Nd}_{10}\text{Fe}_{67}\text{B}_{23})_{95}\text{Nb}_5$  ribbons prepared by melt-spinning technique with different velocity of the copper wheel. Samples in the as-cast state obtained using speed 5 and 10 m/s had nanocrystalline structure. In case of samples prepared by with speed of copper Wheel 15 and 35 m/s were fully amorphous. In the DSC curve, the two minima corresponding to crystallization of the  $\text{Nd}_2\text{Fe}_{23}\text{B}_3$  and  $\text{Nd}_2\text{Fe}_{14}\text{B}$  phases were detected. The coexistence of three phases:  $\text{Nd}_2\text{Fe}_{14}\text{B}$ ,  $\text{Nd}_2\text{Fe}_{23}\text{B}_3$  and  $\text{Nd}_{1-x}\text{Fe}_x\text{B}_4$  were detected. Higher temperatures of annealing caused crystallization of  $\alpha$ -Fe phase. The XRD results were confirmed by the Mössbauer studies.*

*Keywords: hard magnetic materials, phase structure, Mössbauer spectroscopy*

The technology of materials production has strong influence on their microstructure and magnetic properties. Such problem is the fundamental of materials engineering. During materials obtaining process it is necessary to produce sample with required phase composition, which is basic condition to form microstructure. Magnetic properties of material partially depend on phase composition and are formed by microstructure. Proper phase composition guaranties to obtain an optimal magnetic properties and is reached during controlled crystallization in low temperature annealing process [1-3].

The Nd-Fe-B- type compound, in the Fe-rich range, contains following phases [4]:

- hard magnetic  $\text{Nd}_2\text{Fe}_{14}\text{B}$  phase
- B-rich  $\text{Nd}_{1-x}\text{Fe}_x\text{B}_4$  phase
- Nd-rich Nd-Fe phase [5],
- soft magnetic:  $\alpha$ -Fe,  $\text{Fe}_2\text{B}$ ,  $\text{Nd}_2\text{Fe}_{17}$  phases.

The  $\text{Nd}_2\text{Fe}_{14}\text{B}$  compound is characterized by high coercivity  $H_c$ , high density of magnetic energy  $(\text{BH})_{\text{max}}$ , and relatively low the Curie temperature  $T_C=585$  K. The main objective of modification of chemical composition of this compound was an increase of the Curie point. Partial substitution of Fe by Nb causes increasing the  $T_C$  of the  $\text{Nd}_2\text{Fe}_{14}\text{B}$  phase. However, its saturation magnetisation  $J_s$  is decreased while anisotropy field  $H_A$  raises. The chemical compositions of composite permanent magnets are chosen in order to produce biphasic structure based on the  $\alpha$ -Fe –  $\text{Nd}_2\text{Fe}_{14}\text{B}$ . [6-8]. The main goal of present paper was to study of the  $(\text{Nd}_{10}\text{Fe}_{67}\text{B}_{23})_{95}\text{Nb}_5$  alloy.

## Experimental part

Materials to studies was the  $(\text{Nd}_{10}\text{Fe}_{67}\text{B}_{23})_{95}\text{Nb}_5$  alloy. The ingots were prepared by arc-melting of the high purity of constituent elements (more than 3N purity) under low pressure of Ar. Then ribbons were prepared Rusing melt spinning technique under Ar atmosphere. The several linear speeds of copper wheel were used and they equaled 5, 10, 15, and 35 m/s. In order to produce nanocrystalline microstructure, the prepared samples were sealed off in quartz tubes under low pressure of Ar and annealed in the range of temperatures from 923 to 1063K (with step 20K) for 5 min. and then cooled in ice water [9, 10].

Phase structure was investigated using Bruker D8 Advance X0-ray diffractometer with  $\text{CuK}\alpha$  radiation and semiconductor Lynxeye detector. Mössbauer spectra were measured at room temperature using Polon Mössbauer spectrometer working in a transmission geometry with the  $^{57}\text{Co}$  source in the Rh matrix (of the activity of 50 mCi). The studies were carried out on samples crushed to the powder in order to obtain a representation of the entire volume. The analysis was performed using a thin absorber approximation. The Mössbauer spectra were fitted with the WinNORMOS for Igor 6.04 package. Error bars equaled  $\pm 0,1\text{T}$  for hyperfine fields ( $B_{\text{hf}}$ ),  $\pm 0,02$  mm/s for isomeric shifts ( $I_S$ ) or  $\pm 0,05$  mm/s for quadrupole splitting ( $Q_S$ ).

\*email: wnukiza@gmail.com

## Results and discussions

In order to prepare ribbons with different thickness, four different speeds of copper wheel were used Turing melt spinning process. The increase of speed of cooper wheel caused to obtain lower thickness of ribbon: 5m/s – mean ribbon thickness  $d=(60\pm 2)$   $\mu\text{m}$ , 10m/s - mean ribbon thickness  $d=(35\pm 2)$   $\mu\text{m}$ , 15m/s - mean ribbon thickness  $d=(25\pm 2)$   $\mu\text{m}$  and 35 m/s - mean ribbon thickness  $d=(20\pm 2)$   $\mu\text{m}$ .

The X-ray diffraction studies were carried out for all prepared samples of the  $(\text{Nd}_{10}\text{Fe}_{67}\text{B}_{23})_{95}\text{Nb}_5$  alloy in as cast state. The analysis of X-ray pattern (Fig. 1) revealed that in samples with thickness 60, 35, 25 and 20  $\mu\text{m}$ , some reflexes with low intensity are observed, which allowed us to conclude that in samples some crystalline phases present. However, due to low intensity the phases identification was not possible. Moreover, visible braodering of these peaks is related to low volume fraction of these phases and low dimension of grains.

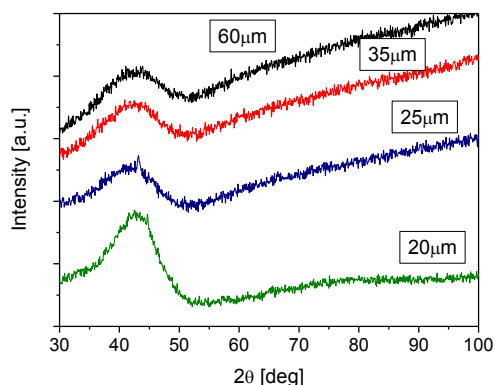


Fig. 1. The X-ray patterns of the  $(\text{Nd}_{10}\text{Fe}_{67}\text{B}_{23})_{95}\text{Nb}_5$  alloys ribbons in the as-cast state

Based on the analysis of the XRD patterns of samples in the as-cast state, the sample obtained using the highest speed of the copper wheel was taken for further studies.

The DSC curve was measured under flow of inert gas (Ar) with a rate of temperature changes 10K/s (Fig. 2). Based on this curve, the temperatures of crystallization begin was revealed  $T_{x1} = 964$  K corresponding to formation of the metastable  $\text{Nd}_2\text{Fe}_{23}\text{B}_3$  phase and  $T_{x2} = 979$  K related to  $\text{Nd}_2\text{Fe}_{14}\text{B}$  phase. Moreover, some other unrecognized peaks were observed. It was helped to reveal temperature range of annealing from 923K to 1063K. Based on results of Zhanga et al [11] and Tamura et al [12], a time of annealing was defined as 5 min.

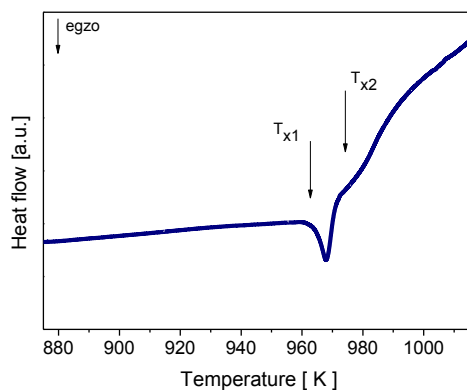


Fig.2. The DSC curve of the amorphous  $(\text{Nd}_{10}\text{Fe}_{67}\text{B}_{23})_{95}\text{Nb}_5$  alloy ribbon.

Then, the samples were annealed in the range of temperatures from 923K to 1063K with step 20K for 5min. in order to produce nanocrystalline microstructure with hard magnetic  $\text{Nd}_2\text{Fe}_{14}\text{B}$  phase. In the next step, we carried out X-ray diffraction of the  $(\text{Nd}_{10}\text{Fe}_{67}\text{B}_{23})_{95}\text{Nb}_5$  alloy ribbons. The analysis of the XRD patterns (Fig. 3) collected for samples annealed at 923K and 943 allowed for identification of hard magnetic  $\text{Nd}_2\text{Fe}_{14}\text{B}$  [13], paramagnetic  $\text{Nd}_{1+\epsilon}\text{Fe}_4\text{B}_4$  [11] and metastable  $\text{Nd}_2\text{Fe}_{23}\text{B}_3$  [14, 15].

The annealing of samples at 963K and higher temperatures caused to nanocrystallization and growth of grains  $\text{Nd}_2\text{Fe}_{14}\text{B}$ ,  $\text{Nd}_2\text{Fe}_{23}\text{B}_3$ ,  $\text{Nd}_{1+\epsilon}\text{Fe}_4\text{B}_4$  phases, while the changes of phase structure was not observed. The phase composition was changed at 1023, 1043 and 1063K (Fig. 4), when additional reflexes corresponding to  $\alpha$ -Fe were detected [11, 12]. The Mössbauer studies confirmed an occurrence of  $\alpha$ -Fe phase in sample annealed at 1063K. The presence of soft magnetic  $\alpha$ -Fe phase in sample annealed at higher temperatures could be related to degradation of the hard magnetic  $\text{Nd}_2\text{Fe}_{14}\text{B}$  phase in this temperature range.

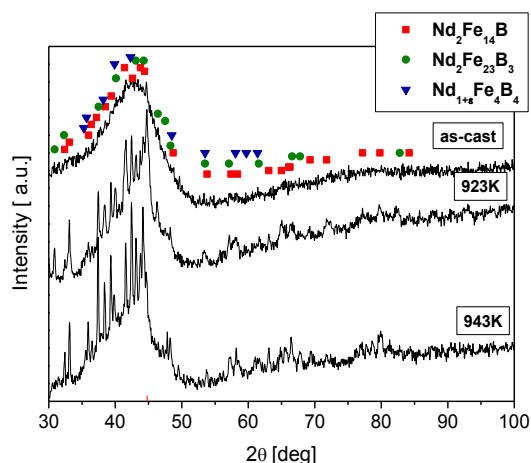


Fig. 3. The XRD patterns of the  $(\text{Nd}_{10}\text{Fe}_{67}\text{B}_{23})_{95}\text{Nb}_5$  alloy ribbons in as-cast state and annealed at 923 and 943K for 5 min.

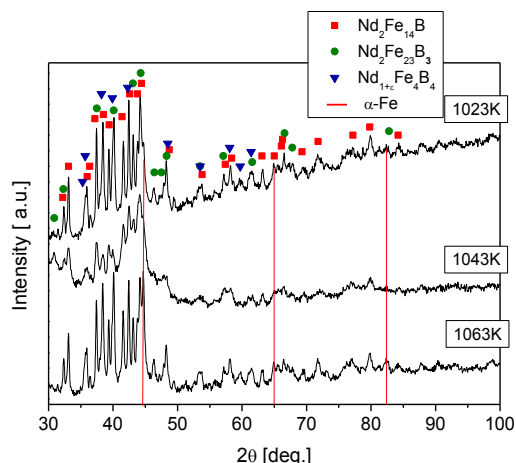


Fig. 4. The XRD patterns  $(\text{Nd}_{10}\text{Fe}_{67}\text{B}_{23})_{95}\text{Nb}_5$  alloy Ribbon annealed at 1023K, 1043K and 1063K for 5 min.

The XRD studies allowed to calculate mean grain size of recognized phases (annealed at 1023K, 1043K and 1063K). In order to reveal mean grain size, the Scherrers method was used [17]. The broadening of diffraction reflexes was used. Scherrers equation was used in following form:

$$D_{hkl} = \frac{K\lambda}{\beta_k \cos \theta_{hkl}} \quad (1)$$

Where:  $K = 0,89$  is the Scherrers constant [18] and  $\lambda = 1,54051 \text{ \AA}$  is wavelength of X-ray radiation [14]. Results of grain size investigation for all samples were collected in Table 1.

**Table 1**  
MEAN GRAIN SIZE  $D_{hkl}$  OF PHASES:  $\text{Nd}_2\text{Fe}_{14}\text{B}$ ,  $\text{Nd}_2\text{Fe}_{23}\text{B}_3$ ,  $\text{Nd}_{1+\epsilon}\text{Fe}_4\text{B}_4$  AND  $\alpha\text{-Fe}$  RECOGNIZED  
IN THE  $(\text{Nd}_{10}\text{Fe}_{67}\text{B}_{23})_{95}\text{Nb}_5$  ALLOY RIBBON ,ANNEALED AT 1023K, 1043K AND 1063K

Phase	Temperature of annelaing		
	1023K	1043K	1063K
$\text{Nd}_2\text{Fe}_{14}\text{B}$	29 nm	26 nm	25 nm
$\text{Nd}_2\text{Fe}_{23}\text{B}_3$	34 nm	32 nm	30 nm
$\text{Nd}_{1+\epsilon}\text{Fe}_4\text{B}_4$	25 nm	23 nm	17 nm
$\alpha\text{-Fe}$	-	-	18 nm

Based on these results it was revealed that the temperature of annealing has not an influence on mean grain size of ferromagnetic  $\text{Nd}_2\text{Fe}_{14}\text{B}$ ,  $\text{Nd}_2\text{Fe}_{23}\text{B}_3$  and  $\alpha\text{-Fe}$  phases. In case of the  $\text{Nd}_{1+\epsilon}\text{Fe}_4\text{B}_4$  phase, a decrease of grain size is observed with an increase of temperature annealing. For sample annealed at 1063 was characterized by the smallest grain size. Al-Khafaji and coworkers [19] investigated the influence of phase composition on magnetic properties of the Nd-Fe-B type alloys produced by melt-spinning. Studies carried out for the  $\text{Nd}_{11,8}\text{Fe}_{82,3}\text{B}_{5,9}$ ,  $\text{Nd}_{9,5}\text{Fe}_{84,5}\text{B}_6$  and  $\text{Nd}_{18}\text{Fe}_{76}\text{B}_6$  alloys revealed that mean grain size was  $\sim 35$  nm for  $\text{Nd}_2\text{Fe}_{14}\text{B}$  phase and  $\sim 15$  nm for  $\alpha\text{-Fe}$ , which corresponds well with results delivered in present work for the  $(\text{Nd}_{10}\text{Fe}_{67}\text{B}_{23})_{95}\text{Nb}_5$  alloy. The nanocrystalline structure of produced samples was confirmed.

The Mössbauer spectroscopy allowed to do more precise identyfication of the  $\text{Nd}_2\text{Fe}_{14}\text{B}$  phase, paramagnetic  $\text{Nd}_{1+\epsilon}\text{Fe}_4\text{B}_4$  phase and metastable  $\text{Nd}_2\text{Fe}_{23}\text{B}_3$  phase in investigated samples. Correct identification based on XRD studies was not possible due to ovaerlapping peaks corresponding to different phases.

In Fig. 5, the Mössbauer spectrum of the  $(\text{Nd}_{10}\text{Fe}_{67}\text{B}_{23})_{95}\text{Nb}_5$  alloy ribbon with thickness 20  $\mu\text{m}$  in the as-cast state. Sample was powdered, in order to investigate its whole volume. The Mössbauer studies were carried out at room temperature. The experimental spectrum was fitted by three subsectrums corresponding to following phases:  $\text{Nd}_2\text{Fe}_{14}\text{B}$ ,  $\text{NdFe}_4\text{B}_4$  and amorphous.

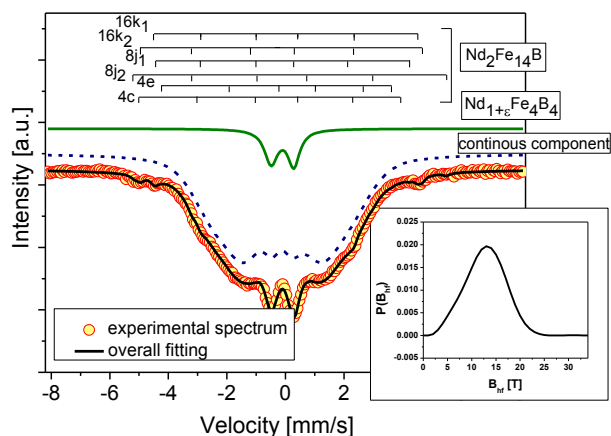


Fig. 5. The Mössbauer spectrum of the  $(\text{Nd}_{10}\text{Fe}_{67}\text{B}_{23})_{95}\text{Nb}_5$  alloy ribbon in the as-cast state with distribution of probability of hyperfine fields  $P(B_{hf})$  corresponding to phases with continuous distribution of hyperfine fields (inset)

The Mössbauer studies of the  $\text{Nd}_{9.5}\text{Fe}_{63.65}\text{B}_{21.85}\text{Nb}_5$  alloy ribbon revealed that material is not fully amorphous. The analysis showed the presence of the hard magnetic  $\text{Nd}_2\text{Fe}_{14}\text{B}$  [20-22]. Moreover, one paramagnetic doublet was assigned to the  $\text{Nd}_{1+\epsilon}\text{Fe}_4\text{B}_4$  phase [23-25].

All parameters of hyperfine structure delivered by the Mössbauer studies were collected in Tab. 2. Moreover, the analysis of the spectrum allowed to determine weight contents of recognized phases. An investigated sample was built by following phases: amorphous (~85 wt.%) and the rest one was  $\text{Nd}_2\text{Fe}_{14}\text{B}$  (3.5 wt.%) phase and  $\text{Nd}_{1+\epsilon}\text{Fe}_4\text{B}_4$  (11.1 wt.%).

In Fig. 6, the Mössbauer spectra registered for the  $(\text{Nd}_{10}\text{Fe}_{67}\text{B}_{23})_{95}\text{Nb}_5$  alloy ribbon, annealed at 1043K (a) and 1063K (b) for 5 min. together with distribution of hyperfine fields  $P(B_{hf})$  corresponding to theoretical curve. During spectrum analysis, contributions from the hard magnetic  $\text{Nd}_2\text{Fe}_{14}\text{B}$ , paramagnetic  $\text{Nd}_{1+\epsilon}\text{Fe}_4\text{B}_4$  and metastable  $\text{Nd}_2\text{Fe}_{23}\text{B}_3$  were considered. The paramagnetic  $\text{Nd}_{1+\epsilon}\text{Fe}_4\text{B}_4$  phase was described by single doublet. The presence of the  $\text{Nd}_2\text{Fe}_{14}\text{B}$  phase is represented by six Zeeman sextets corresponding to six nonequivalent positions of Fe atoms in the elementary cell. Moreover, during calculations, three Zeeman sextets were assigned to the metastable soft magnetic  $\text{Nd}_2\text{Fe}_{23}\text{B}_3$  phase [26-28]. In order to increase accuracy of fitting, the additional line corresponding to continuous distribution of the hyperfine fields was added. This line is related to the presence of disordered phase.

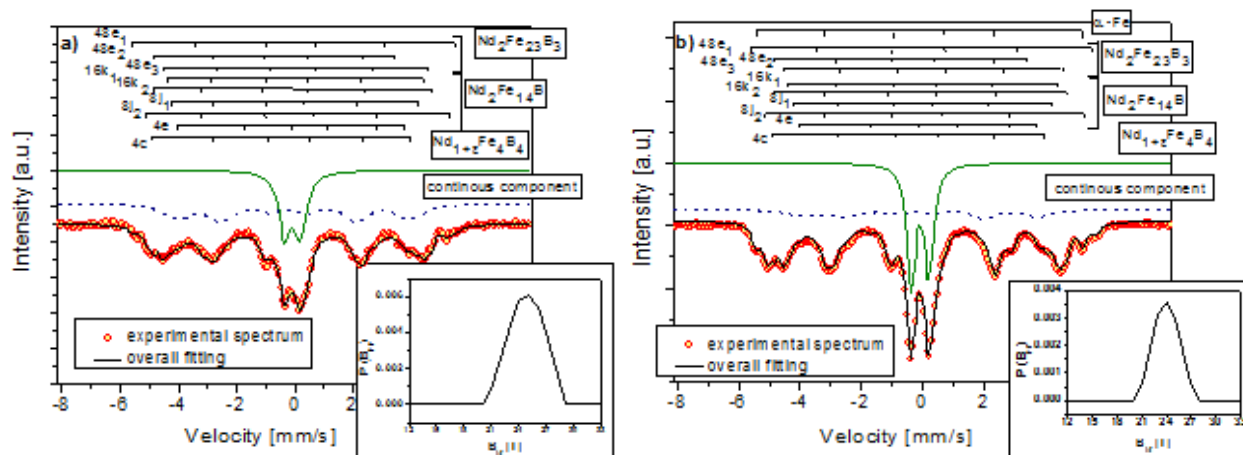


Fig. 6. The Mössbauer spectra of the  $(\text{Nd}_{10}\text{Fe}_{67}\text{B}_{23})_{95}\text{Nb}_5$  alloy Ribbon annealed at 1043K (a) and 1063K (b) for 5 min. together with distribution of hyperfine fields  $P(B_{hf})$  corresponding to phases with continuous distribution of hyperfine fields.

In Table 2 volume contents of recognized phases in the sample of  $(\text{Nd}_{10}\text{Fe}_{67}\text{B}_{23})_{95}\text{Nb}_5$  were collected. An increase of annealing temperature, the rise of volume content of crystalline phases is observed at the expense of disordered phase. In case of sample with temperature of heat treatment 1063K, the presence of small amount of the soft magnetic  $\alpha\text{-Fe}$  phase (about 3 wt.%) [23, 29-31], which was not observed at lower temperatures.

**Table 2**  
VOLUME CONTENTS OF RECOGNIZED PHASES IN THE  $(\text{Nd}_{10}\text{Fe}_{67}\text{B}_{23})_{95}\text{Nb}_5$  ALLOY RIBBONS,  
IN THE AS-CAST STATE AND ANNEALED AT 1043K AND 1063K FOR 5 MIN.

	V [wt. %]		
	As-cast state	1043K	1063K
$\text{Nd}_2\text{Fe}_{14}\text{B}$	3.5	21.3	30.1
$\text{Nd}_2\text{Fe}_{23}\text{B}_3$		9.1	11.7
$\text{Nd}_{1+\epsilon}\text{Fe}_4\text{B}_4$	11.1	40.2	42.6
$\alpha\text{-Fe}$			2.9
Disordered phase	85.4	29.4	12.7

The Mössbauer studies revealed changes in phase constitution during heat treatment. Percentage content of the hard magnetic  $\text{Nd}_2\text{Fe}_{14}\text{B}$  phase has a strong influence on values of magnetic parameters of produced sample. Moreover, the presence of paramagnetic phase in sample affects on the saturation magnetization and maximum density of magnetic energy.

### Conclusions

The analysis of the XRD patterns revealed that heat treatment causes changed in the structure of crystalline ribbon. The recognized phases were  $\text{Nd}_2\text{Fe}_{14}\text{B}$ ,  $\text{Nd}_{1+\epsilon}\text{Fe}_4\text{B}_4$ ,  $\alpha\text{-Fe}$  (this phase was observed at 1063K). Moreover, short time annealing allowed to form metastable  $\text{Nd}_2\text{Fe}_{23}\text{B}_3$  phase, which proves nanocrystalline structure. An increase of temperature caused an increase of the percentage content of crystalline phases. The sample in the as-cast state was generally built by amorphous phase (85 wt.%), with small amount of the hard magnetic  $\text{Nd}_2\text{Fe}_{14}\text{B}$  phase (3.5 wt.%) and paramagnetic  $\text{Nd}_{1+\epsilon}\text{Fe}_4\text{B}_4$  phase (11.1 % wag.). For sample annealed at 1063K, the content of desired hard magnetic  $\text{Nd}_2\text{Fe}_{14}\text{B}$  phase rises to ~30.1 wt.% to 3.5 wt.% for sample in as-cast state.

### References

- GARUS, S., NABIAŁEK, M., GARUS, J., Acta Phys. Pol. A **126**, 2014, p. 961.
- NABIAŁEK, M., Archives of Metallurgy and Materials, **60**, 2015, p. 1988.
- NABIAŁEK, M., J. All. Compd. **642**, 2015, p. 98.
- BAUER, J., SEEGER, M., ZERN, A., KRONMÜLLER, H., J. Appl. Phys., **80**, 1996, p. 1667.
- ZBROSZCZYK, J., FUKUNAGA, H., OLSZEWSKI, J., CIURZYŃSKA, W. H., HASIAK, M., BŁACHOWICZ, A., J. Magn. Magn. Mater. **215-216**, 2000, p. 41921.
- KIRCHMAYR, H. R., J. Phys.D: Appl. Phys. **29**, 1996, p. 2763.
- SCHNEIDER, G., HENIG, E. TH., PETZOW, G., STADELMAIER, H. H., Zeitschrift für Metallkunde, **77**, 1986, p. 755.
- SEEGER, M., KRONMÜLLER, H., Zeitschrift für Metallkunde **87**, 1996, p. 923.
- PRZYBYŁ, A., PAWLIK, K., PAWLIK, P., GĘBARA, P., WYSŁOCKI, J.J., J. All. Compd. **536**, 2012, p. 333.
- ZHANG, J., LIM, K.Y., FENG, Y.P., LI, Y., Scripta Materialia **56**, 2007, p. 943.
- TAMURA, R., KOBAYASHI, S., FAKUZAKI, T., ISOBE, M., UEDA, Y., Journal of Physics: Conference Series **144**, 2009, art. 012068.
- HERBST, J.F., Reviews of Modern Physics, **63**, No. 4, 1991, p. 819.
- YARTYS, V.A., GUTFLEISCH, O., HARRIS, I.R., Journal of Magnetism and Magnetic Materials **157/158**, 1996, p. 119.
- MAYOT, H., ISNARD, O., SOUBEZROUX, J.L., Journal of Magnetism and Magnetic Materials, **316**, no. 2, 2009, p.e477.
- GOU, C., CHENG, Z.X., CHEN, D.F., NIU, S.W., YAN, Q.W., ZHANG, P.L., SHEN, B.G., YANG, L.Y., J. Magn. Magn. Mater., **128**, 1993, p.26.
- BOJARSKI, Z., ŁĄGIEWKA, E., *Rentgenowska analiza strukturalna*, Wydawnictwo Uniwersytetu Śląskiego, Katowice 1995.
- SZWAJA, M., GĘBARA, P., FILIPECKI, J., PAWLIK, K., PRZYBYŁ, A., PAWLIK, P., WYSŁOCKI, J.J., FILIPECKA, K., J. Magn. Magn. Mater. **382** 2015 p.307.
- AL-KHAFI, M.A., RAINFORTH, W.M., GIBBS, M.R.J., DAVIES, H.A., BISHOP, J.E.L., J. Magn. Magn. Mater. **188**, 1998, p.109.
- HÜTTEN, A., JOM, **44**, 1992, p.11.
- HERBST, J.F., CROAT, J.J., PINKERTON, F. E., Physical Review B, **29**, 1984, p.4176, DOI:10.1103/PhysRevB.29.4176.
- PLUSA, D., WYSŁOCKI, J.J., WYSŁOCKI, B., PFRANGER, R., Journal of the Less-Common Metals, **133**, 1987, p. 231.
- STEYAERT, S., LE BRETON, J.M., AHMED, F.M., EDGLEY, D.S., HARRIS, I.R., TEILLET, J., J. All. Compd. **264**, 1998, p.277.
- GUTFLEISCH, O., J. Phys. D: Appl. Phys. **33**, 2000 p.R157.
- RODEWALD, W., KATTER, M., WALL, B., BLANK, R., REPEL, G.W., ZILG, H.D., IEEE Trans. Mag. **36**, 2000, p.3279.
- NASU, S., HINOMURA, T., HIROSAWA, S., KANEKIYO, H., Physica B **237-238**, 1997, p.283.
- TILJAN, N., ZAK, T., STAJIC-TROSIC, J., MENUSHENKOV, V., Metalurgija-Journal of Metallurgy, **8**, 2002, p.201.
- CHENG, Z., SHEN, B., ZHANG, J., MAO, M., SUN, J., YANG, CH., Chin. Phys. Lett. **14 (5)**, 1997, p.387.
- POPOW, A.G., SERIKOV, V.V., KLEINERMAN, N.M., The Physics of Metals and Metallography, **109 (5)**, 2010, p.505.
- YAMASAKI, M., HAMANO, M., KABAYASHI, T., Materials Transactions, **43 (11)**, 2002, p.2885.
- YANG, CH. J., HAN, J. S., PARK, E.B., KIM, E.CH., J. Magn. Magn. Mater. **301**, 2006, p.220.
- GONDRO, J., BŁOCH, K., NABIAŁEK, M., Acta Physica Polonica A, **130**, 2016, p. 909.

Manuscript received: 11.12.2019